bands and gap states from optical absorption and electron-spin-resonance studies on amorphous carbon and amorphous hydrogenated carbon films

π bands and gap states from optical absorption and electron-spin-resonance studies on amorphous carbon and amorphous hydrogenated carbon films

D. Dasgupta,* F. Demichelis, C. F. Pirri, and A. Tagliaferro
Dipartimento di Fisica, Politecnico di Torino, Torino, Italy
(Received 2 August 1990)

Amorphous carbon a-C and amorphous hydrogenated carbon a-C:H films were prepared by rf sputtering of a graphite target in argon and argon-plus-hydrogen atmospheres, respectively. The optical-absorption coefficients of these films were measured by a spectrophotometer in the high-absorption range and by photothermal deflection spectroscopy in the low-absorption range. They were also studied by electron-spin-resonance (ESR) measurements. The optical-absorption spectrum is found to have a rather broad peak, in contrast to the sharp rise in absorption near the band gap observed for normal semiconductors. To explain this broad peak, a model density of states (DOS) for these materials is proposed, in accordance with their well-known microstructure. This consists of a pair of broad Gaussian-like distributions lying above and below the Fermi level and separated by about 4 eV, arising out of the π states of the aromatic sixfold rings that comprise the bulk of the graphitic sp^2 regions, as well as pairs of discrete levels that are about 0.6 eV apart and are produced by fivefold and sevenfold rings present in these regions. The proposed DOS explains the essential features of the optical-absorption spectra and ESR data. The validity of the concept of the optical gap for these materials is also discussed.

INTRODUCTION

Amorphous carbon a-C and amorphous hydrogenated carbon a-C:H have been attracting a great deal of interest in the last few years.[1,2] Valuable information on their properties and structures can be obtained by analyzing absorption-coefficient data in the NIR-visible-UV region and from electron-spin-resonance (ESR) signals.

However, the information is often looked at in light of existing models for amorphous semiconductors. In a typical amorphous semiconductor, such as a-Si:H, the electronic states can be divided into three types: extended, band tails, and deep states.[3] Each of these originates from a different physical process: extended states from long-range correlation and symmetry, tail states from structural disorder, and deep states by structural defects. While deep states can be investigated by means of the ESR technique, information about the states lying near band edges is more difficult to obtain. Since in amorphous semiconductors the gap between conduction and valence bands is filled with states, the concept of gap, as used in crystalline materials, is modified. While there is no gap in the sense of an energy region lacking states, a mobility gap exists, since the mobility in extended (band) and localized (tail) states is different by orders of magnitude.[3] The band edges are now looked at as the energies at which a transition from extended to localized states occurs. However, while the determination of the exact position of the mobility edges is difficult, if at all possible, the extraction of the value of the so-called optical gap[2] E_g from the absorption-coefficient energy dependence is a routine procedure. The fact that the optical gap is nevertheless a good indicator of the band spacing is strictly correlated to the different origin of extended and localized states and to the consequent different shapes of the density of states (DOS) over and below band edges. This difference is clearly reflected in the sharp change of slope of the $\log_{10}\alpha$ versus E curves near E_g for a-Si:H and its alloys.[4] Although it is customary[2] to use the concept of optical gap and the same procedure used for a-Si:H for its evaluation also when a-C and a-C:H are concerned, it is not at all obvious that its physical meaning is the same.

First of all, in this case we are dealing with a mixed σ, π-bonded system in which the σ-σ^* energy spacing is expected to be around 5 eV,[2] so that, as far as ESR and optical absorption below 4 eV are concerned, they can be neglected indeed.

Moreover, the π-π^* states, which are less separated in energy, are originated by aromatic rings joined together to form graphiticlike islands.[2] The width of the peaks in the DOS corresponding to these states is correlated to the distribution of island sizes, with larger islands giving rise to closer π-π^* couples.[2] Even if we admit that some of these states are localized and some extended, it is clear that there is no difference in their physical origin. As a consequence, if one looks at the $\log_{10}\alpha$ versus E curves in a-C and a-C:H, one can clearly observe the lack of the sharp feature of a-Si:H, substituted by a somewhat smooth change in slope.[1,2,5,6]

The aim of this paper is to analyze the $\log_{10}\alpha$ versus E curves for a-C and a-C:H of samples deposited by sputtering of a carbon target in an Ar atmosphere, without and with H_2 flow, and the spin densities as obtained by ESR. An attempt to obtain a DOS model which is in agreement with optical absorption and ESR data is made.

Absorption data were obtained by NIR-visible-UV spectroscopy and photothermal deflection spectroscopy

(PDS). The details of the Tauc model for the optical gap in amorphous semiconductors and the limit of its applicability are discussed. It is shown, through the evaluation of the absorption coefficient, that a sharp change in the DOS shape near band edges is not necessary to explain the linearity of the Tauc plot. Instead, broad π and π^* peaks, assumed to be Gaussian for simplicity, can explain the shape and magnitude of the absorption coefficient.

The expected contribution of these peaks to the ESR signal, obtained by extending the Gaussian bands up to the Fermi level, is much lower than the experimentally observed signal, hence another possible contribution to the ESR signal (arising from oddfold rings) is considered and justified.

Finally, a sketch of the DOS relevant to determine the optical and spin properties of *a*-C and *a*-C:H is made and shown to be in agreement with literature data for *a*-C and sp^2-rich *a*-C:H.

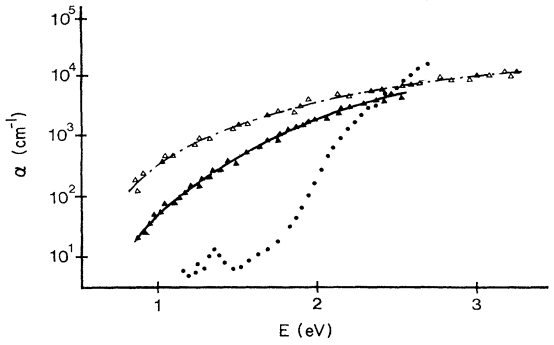

FIG. 1. Plot of the optical-absorption coefficient (α) as a function of photon energy (E) for two of our samples along with theoretical curves obtained by fitting with Eq. (5) (see text). A plot of α for an *a*-SiC:H sample is also shown for comparison. *CH*05: ▲ (experimental), —— (theoretical). *C*500: △ (experimental), —·—·— (theoretical). *a*-Sic:H (10 at. % C): ● (experimental)

FILM DEPOSITION AND ANALYSIS

The films were deposited at room temperature by rf sputtering of a carbon cathode (purity 99.999%; 20 cm in diameter) in an Ar (*a*-C) or Ar-H_2 (*a*-C:H) atmosphere. For *a*-C samples, Ar flow rate was set at 80 SCCM (where SCCM denotes cubic centimeter per minute at STP), pressure was kept at 3.3 Pa, and rf power varied from 300 to 500 W. For *a*-C:H films, the same Ar flow rate and pressure were used, rf power was fixed at 300 W, and hydrogen flow rate varied from 5 to 35 SCCM.

In the following, *a*-C samples are labeled with a *C* followed by rf power in watts and *a*-C:H by *CH* followed by hydrogen flow rate in SCCM. It should be noted that sample *C*300 could also be designated as *CH*00.

Hydrogen content was estimated by elastic recoil detection analysis (ERDA) measurements and carbon content by Rutherford backscattering spectroscopy: CH samples were found to contain approximately 30 at. % of H. Optical measurements were recorded on a Perkin Elmer UV-visible-NIR Lambda 9 Spectrophotometer in the 0.4–1.6-μm range.

The absorption coefficient in the high-absorption region was extracted from optical measurements following the procedure reported in Ref. 7. In the low-absorption region, $\alpha < 10^4$ cm^{-1}, it was obtained by means of PDS measurements.[8] ESR measurements were carried out by a Varian EPR 109 spectrometer on films deposited on quartz substrates at room temperature, with an incident power less than 1 mW in order to prevent saturation. The absolute spin density and g shift were obtained by comparison with diphenylpicrylhydrazyl (DPPH) standard sample ($g = 2.0036$) and Varian pitch ($g = 2.0029$).

EXPERIMENTAL RESULTS

Figure 1 reports the experimentally observed absorption-coefficient curves and the fitting curves (obtained as specified below) for two of our samples: as mentioned in the Introduction, no sharp changes of slope are observed, but only broad shoulders. A typical curve for *a*-SiC:H is also shown, in order to emphasize the difference between the two types of absorption curves.

Figure 2 shows the $\sqrt{\alpha(E)E}$ versus E plot of the data in the high-absorption region and their linear interpolation, following the standard procedure set by Tauc[9] for the extraction of the optical gap. Again, the difference between our samples and *a*-SiC:H is quite prominent. Especially, the larger departure from the interpolating line in our samples with respect to *a*-SiC:H and the different slope of the line should be noted.

In the following paragraphs, we attempt to explain the above-quoted differences in behavior among *a*-C, *a*-C:H, and *a*-SiC:H in terms of the standard theory for optical absorption in amorphous semiconductors, making use of the fact that in *a*-C and *a*-C:H, levels corresponding to the π and π^* states are present which have no counterpart for *a*-Si.

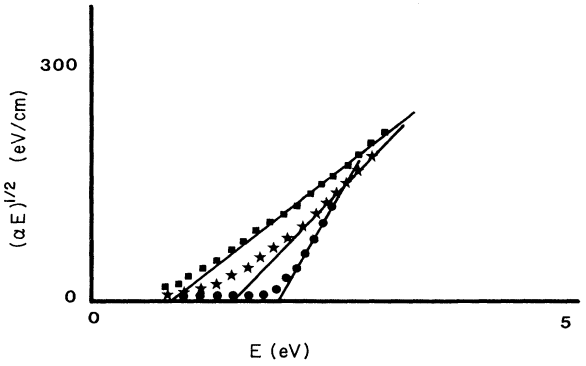

FIG. 2. Plot of $(\alpha E)^{1/2}$ against E for the same samples as in *CH*05, ★; *C*500, ■; *a*-SiC:H, ●.

ABSORPTION COEFFICIENT AND TAUC GAP

The fundamental quantity correlated to the DOS is the imaginary part of the dielectric constant. For nondirect optical transitions and within the one-electron approximation, it is given, at 0 K, by[10]

$$\epsilon_2(E)=\left[2\pi e\frac{\hbar^2}{m}\right]^2\left[\frac{Q}{E}\right]^2\frac{4}{\nu\rho_a}\times\int_{E_f}^{E_f+E}N_0(Z-E)N_u(Z)dZ\ , \tag{1}$$

where E is the photon energy, e is the electronic charge, ν the numbers of valence electrons per atom, ρ_A the atomic density, N_0 the density of occupied states, N_u the density of unoccupied states, and Q the matrix element of the optical transition. Since absorption coefficient $\alpha(E)$ is given by

$$\alpha(E)=\frac{2\pi}{hcn}E\epsilon_2(E)\ , \tag{2}$$

where n is the refractive index, h the Planck constant, and c the speed of light, we can write

$$\alpha(E)=\frac{K}{E}\int_{E_f}^{E_f+E}N_0(Z-E)N_u(Z)dZ\ , \tag{3}$$

where K is defined as

$$K=\frac{(2\pi)^3e^2\hbar^3}{m^2cn}Q^2\frac{4}{\nu\rho_\alpha}\ .$$

To work out the expression for the optical gap, Tauc assumed a parabolic behavior of the bands near the edges and a constant momentum transition, so obtaining

$$\alpha(E)E=B(E-E_g)^2\ , \tag{4}$$

which is represented, on a $\sqrt{\alpha(E)E}$ versus E plot, by a straight line that intercepts the E axis for $E=E_g$, since B is a constant. Although the assumptions leading to the Tauc relation may not be fulfilled, plots of $\sqrt{\alpha(E)E}$ versus E for a-C and a-C:H show a linear zone and the Tauc gap has provided a simple parametrization of the absorption edge.

Since in a-C and a-C:H the broadening of the π and π^* is correlated to the distribution of island size, we will assume, as a first approximation, a Gaussian form for the bands. For the sake of simplicity, we assume the bands to be symmetric with respect to Fermi level (set as the zero of the energy scale: $E_\pi=-E_{\pi^*}$)

$$N_0(E')=N_{\pi\max}\exp\left[-\frac{(E'-E_\pi)^2}{2\sigma^2}\right]\ ,$$

$$N_u(E'')=N_{\pi\max}\exp\left[-\frac{(E''-E_{\pi^*})^2}{2\sigma^2}\right]\ .$$

Substituting in Eq. (3) and integrating, we find that

$$\alpha(E)=K\sqrt{\pi}\sigma N_{\pi\max}^2\exp\left[-\left[\frac{2E_{\pi^*}-E}{2\sigma}\right]^2\right]\times\frac{\mathrm{erf}[E/(2\sigma)]}{E}\ . \tag{5}$$

As can readily be observed, the shape of the absorption coefficient is determined only by E_{π^*} and σ, that is, the position and width of the peaks. The Tauc function is given by

$$\sqrt{\alpha(E)E}=C\exp\left[-\frac{1}{2}\left[\frac{2E_{\pi^*}-E}{2\sigma}\right]^2\right]\sqrt{\mathrm{erf}[E/(2\sigma)]}\ , \tag{6}$$

where C is defined as

$$C=(K\sqrt{\pi}\sigma N_{\pi\max}^2)^{1/2}\ .$$

The exponential factor is a Gaussian centered at $E=2E_{\pi^*}$ and having a width of 2σ. In the low-energy region a deformation of the Gaussian is caused by the presence of the error function. A quasilinear behavior is expected near the point of inflection, so that a line having as slope the derivative of the function in such a point will be a good approximation of the curve over a wide range of energies.

To check if the assumption of Gaussian bands is sufficient to explain both the absorption curve and the Tauc gap values obtained, we will proceed in the following way.

(1) Fitting of the absorption curve in the low-absorption region by means of Eq. (5), in order to obtain the parameters of the Gaussian bands and the factor C.

(2) Use of the parameters so obtained to generate, by means of Eq. (6), the $\sqrt{\alpha(E)E}$ curve in the high-absorption region.

(3) Determination of the Tauc parameters B' and E_g' and their comparison with the ones obtained analyzing optical-abosrption experimental data.

The application of this procedure leads us to the results reported in Table I, where B and E_g are the experimental values and B' and E_g' those obtained as specified above, and to the fitting curves of Fig. 1. The two curves shown correspond to samples with the lowest and highest values of absorption. It is clear from that figure that the fitting curves are well approximating experimental data.

The values in Table I show the accuracy of the approach, since only departure from the measured values of less than $\frac{1}{10}$ of an eV for E_g and about 20% for B are observed. These values have to be compared with the nonrealistic, as expected, estimates obtained by applying the above-quoted procedure to the a-SiC:H curve of Fig. 1.

It can also be observed that, while the shape of the absorption coefficient is determined, as said above, only by E_{π^*} and σ, its absolute value is also determined by the parameters of Eq. (5). Assuming reasonable values of the parameters ($\nu=1$, since only π electrons are involved; $\rho=1.5$, g/cm^3, from which ρ_A is obtained; n as measured; $N_{\pi\max}=10^{22}$ states/eV cm^3) the curves can be fitted using values of the matrix element of a few Å, fully compatible with theoretical estimates. If one instead uses the standard value for the DOS at the band edges ($N_c=5\times10^{21}$ states/eV cm^3) and inserts it in the appropriate expression for parabolic band edges,[9] it turns out that the matrix element is of the order of some tens of Å, too large to be acceptable.[9]

TABLE I. Tauc and Gaussian parameters.

Sample	E_π (eV)	σ (eV)	E_g' (eV)	B' $(\text{eV cm})^{-1}$	E_g (eV)	B $(\text{eV cm})^{-1}$
*C*300	1.72	0.50	1.44	1.11×10^4	1.46	1.41×10^4
*C*350	1.72	0.60	1.06	1.38×10^4	0.97	1.18×10^4
*C*400	1.85	0.67	1.05	1.42×10^4	0.98	1.18×10^4
*C*440	1.65	0.50	1.30	1.43×10^4	1.24	1.00×10^4
*C*500	1.75	0.65	0.94	1.52×10^4	0.90	0.93×10^4
*CH*05	1.75	0.50	1.50	1.23×10^4	1.45	1.00×10^4
*CH*12.5	1.62	0.48	1.32	1.21×10^4	1.37	1.29×10^4
*CH*20	1.95	0.73	1.23	1.18×10^4	1.24	1.12×10^4
*CH*27.5	1.60	0.50	1.20	1.38×10^4	1.21	1.30×10^4
*CH*35	1.80	0.60	1.21	1.43×10^4	1.18	1.00×10^4
a-SiC:H	2.17	0.36	2.9	3.18×10^5	2.00	1.00×10^5

Although the Gaussian shape of the bands is only a first-order approximation, it gives convincing results, so that one can observe the following.

(a) There is no difference in the origin of the states sitting below and above the "optical band edges."

(b) Since only the shape and position of the Gaussian affect the E_g' value, there is no direct connection between the "mobility gap," the distance between the thresholds dividing localized from extended states, and the value of the optical gap. Instead, the localization is correlated to the number of states at a given energy, that is, to both the height and the shape of the peaks.

(c) As a limiting case, the π and π^* bands can be completely localized and still an optical gap will be obtained from the Tauc plot.

(d) The optical gap value is a purely indicative parameter, when a characterization of the material is looked for.

(e) E_{04} [the energy value at which $\alpha(E)=10^4\ \text{cm}^{-1}$], customarily used as an alternative to the Tauc gap, is even less significant, since no relation can be traced to significant characteristics of the material (observe the absolute values of α in Fig. 1 and compare with the values of Table I).

Since larger islands give rise to closer π-π^* couples and only infinite islands can produce sixfold states at Fermi level,[2] π and π^* bands will not reach Fermi level. A faster decrease than Gaussian as the Fermi level is approached is then expected. As a consequence, no significant contribution to the ESR signal from the tails of the bands is foreseen. Anyhow, using the parameters of Table I and the Fermi-Dirac function, the number of unpaired spins can be estimated and are found to be well below measured values. To explain the ESR signal, then, contribution from other states has to be considered.

ORIGIN OF ESR SIGNALS

In amorphous tetrahedral semiconductors the excess absorption coefficient, obtained by integrating the residual absorption coefficient (after subtraction of the exponential component) down to the low-energy limit of the spectrum, is related to the spin density measured by ESR.[4,11] Hence both ESR and PDS can give the same information on uncharged defects. Such a relation is not expected to exist in *a*-C and *a*-C:H.

In Table II we report values of the spin density (N_s), g values, and peak-to-peak amplitudes (δH_{PP}) for all the samples. In every case, a spin-density value of over $10^{19}/\text{cm}^3$ was obtained. These values are too high to be derived from the Gaussian tails of π bands as introduced above. Probably these arise from fivefold and sevenfold aromatic rings with unpaired electrons lying near the Fermi level.[2]

The presence of such gap states has negligible influence on the α versus $h\nu$ curves, unlike in usual amorphous semiconductors, because of the broad Gaussian shape of the π and π^* bands in this case. In Table II we can also observe a difference of two orders of magnitude in N_s between hydrogenated and nonhydrogenated samples. The reason could be that H partially saturates the dangling bonds, or, by decreasing coordination number, releases internal stress responsible for unpaired spins.

Saturation measurements were also performed on all samples. In a previous work[12] saturation was observed for *a*-C:H samples with about 10^{18} spins/cm^3 and explained by the delocalization effects and low spin-lattice coupling of the unpaired electrons. In this case, we have observed saturation at about 5 mW only in the sample with the lowest N_s, while all the other samples showed no saturation up to a power level of 30 mW. Probably a high value of N_s implies a strong spin-spin coupling which would prevent saturation.

TABLE II. ESR parameters.

Sample	N_s (cm^{-3})	g	ΔH_{PP} (10^{-4} T)
*C*300	6×10^{20}		6
*C*350	1×10^{21}	2.0035	7
*C*400	1×10^{21}	2.0029	10
*C*440	8×10^{20}	2.0030	7
*C*500	9×10^{20}	2.0023	8.5
*CH*05	1×10^{19}		8.5
*CH*12.5	1×10^{20}	2.0026	7.5
*CH*20	8×10^{19}	2.0026	5.5
*CH*27.5	1×10^{20}	2.0023	7
*CH*35	2×10^{20}	2.0023	4.5

NATURE OF THE DENSITY-OF-STATES CURVE

From the above discussion, the density-of-states distribution near the fundamental absorption edge of *a*-C and *a*-C:H would be seen to arise from two distinct contributions.

(a) Two broad peaks, approximately Gaussian, separated by about 4 eV and lying on opposite sides of the Fermi level, produced by sixfold rings making up the bulk of the graphitic (sp^2) islands.

(b) A number of discrete levels, lying about 0.3 eV above and below the Fermi level, produced by odd fivefold and sevenfold rings within these islands.

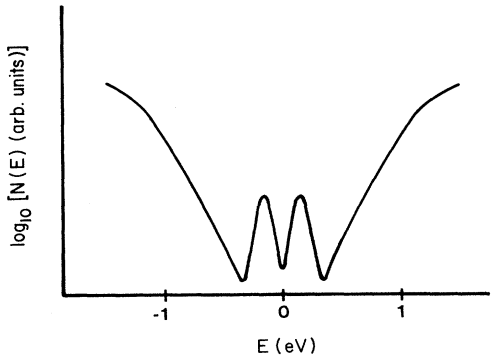

FIG. 3. Schematic diagram of the proposed density-of-states [$N(E)$] curve for *a*-C and *a*-C:H. The zero on the energy scale corresponds to the position of the Fermi level.

States which make up part (a) above are responsible for most of the observed optical absorption, while those in (b) give rise to the ESR signals as also the conductivity near room temperature.[13] A schematic diagram of the proposed density of states is given in Fig. 3.

The above arguments apply, of course, only in those situations where there is a significant proportion of π and π^* states, that is, where a large fraction of the material is composed of graphitic islands. If this is not the case, the above states would contribute little to the optical absorption, which will now be dominated by electronic transitions between the tail states of σ and σ^* corresponding to the sp^3 regions.

CONCLUDING REMARKS

a-C and *a*-C:H samples have been prepared and studied by optical and ESR measurements. In order to explain the observed results, a simple model for the DOS has been developed. Two distinct contributions to the DOS are proposed, one from a Gaussian-like distribution of π and π^* states arising from sixfold rings, while the other, composed of discrete levels, is expected to appear due to the presence of both fivefold and sevenfold rings present in the graphitic islands. It has been demonstrated that such a model can satisfactorily explain optical-absorption data as well as those obtained from ESR measurements.

*On leave from North Bengal University, Siliguri, India.

[1]J. C. Angus, P. Koidl, and S. Domitz, in *Plasma Deposited Thin Films,* edited by J. Mort and F. Jansen (CRC, Boca Raton, FL, 1986), Chap. 4.

[2]J. Robertson, Adv. Phys. **35**, 317 (1986).

[3]E. A. Davis and N. F. Mott, Philos. Mag. **22**, 903 (1970).

[4]W. B. Jackson and N. M. Amer, Phys. Rev. B **25**, 5559 (1982).

[5]J. J. Hauser, J. Non-Cryst. Solids **23**, 21 (1977).

[6]B. Dischler, A. Bubenzer, and P. Koidl, Appl. Phys. Lett. **42**, 636 (1983).

[7]F. Demichelis, G. Kaniadakis, A. Tagliaferro, and E. Tresso, Appl. Opt. **26**, 1737 (1987).

[8]N. M. Amer and W. B. Jackson, in *Semiconductors and Semimetals,* edited by J. I. Pankove (Academic, New York, 1984), Vol. 21B, Chap. 3.

[9]J. Tauc, R. Grigorovici, and A. Vancu, Phys. Status Solidi **15**, 627 (1966).

[10]G. Cody, in *Semiconductors and Semimetals,* edited by J. I. Pankove (Academic, New York, 1984), Vol. 21B, Chap. 2.

[11]F. Demichelis, C. F. Pirri, E. Tresso, and G. Amato, Thin Solid Films (to be published).

[12]R. J. Gambino and J. A. Thompson, Solid State Commun. **34**, 15 (1970).

[13]D. Dasgupta, F. Demichelis, and A. Tagliaferro, Philos. Mag. B (to be published).